



ISSN 1476-8186

Volume 3
Number 4
October 2006

CA

International Journal of
**AUTOMATION
AND
COMPUTING**



INSTITUTE OF AUTOMATION, CHINESE ACADEMY OF SCIENCES



CHINESE AUTOMATION AND COMPUTING SOCIETY IN THE UK

A PUBLICATION OF

International Journal of Automation and Computing

Volume 3 Number 4

October 2006

Table of Contents

Guest Editorial

Special Issue on Biologically Inspired Robotic Fish

Learning from Fish: Kinematics and Experimental Hydrodynamics for Roboticists	<i>G. V. Lauder, P. G. A. Madden</i>	325
Biologically Inspired Behaviour Design for Autonomous Robotic Fish	<i>J. D. Liu, H. Hu</i>	336
Locomotion and Depth Control of Robotic Fish with Modular Undulating Fins	<i>K. H. Low</i>	348
A New Type of Hybrid Fish-like Microrobot	<i>W. Zhang, S. X. Guo, K. Asaka</i>	358
Bio-inspired Actuating System for Swimming Using Shape Memory Alloy Composites	<i>T. Tao, Y. C. Liang, M. Taya</i>	366
A Computational Fluid Dynamics (CFD) Analysis of an Undulatory Mechanical Fin Driven by Shape Memory Alloy	<i>Y. H. Zhang, J. H. He, J. Yang, S. W. Zhang, K. H. Low</i>	374
Development of ICPF Actuated Underwater Microrobots	<i>X. F. Ye, B. F. Gao, S. X. Guo, L. Q. Wang</i>	382

Regular Papers

Using the Correlation Criterion to Position and Shape RBF Units for Incremental Modelling	<i>X. X. Wang, S. Chen, C. J. Harris</i>	392
Stability and Stabilization of Block-cascading Switched Linear Systems	<i>Y. H. Zhu, D. Z. Cheng</i>	404
Data Transfer Over the Internet for Real Time Applications	<i>C. W. Dai, S. H. Yang, R. Knott</i>	414
A New Smoothing Approach with Diverse Fixed-lags Based on Target Motion Model	<i>C. Li, C. Z. Han, H. Y. Zhu</i>	425

Development of ICPF Actuated Underwater Microrobots

Xiu-Fen Ye*, Bao-Feng Gao

Automation College, Harbin Engineering University, Harbin 150001, PRC

Shu-Xiang Guo

Automation College, Harbin Engineering University, Harbin 150001, PRC
Faculty of Engineering, Kagawa University, Takamatsu 761-0396, Japan

Li-Quan Wang

College of Mechanical Electrical Engineering, Harbin Engineering University, Harbin 150001, PRC

Abstract: It is our target to develop underwater microrobots for medical and industrial applications. This kind of underwater microrobots should have the characteristics of flexibility, good response and safety. Its structure should be simple and it can be driven by low voltage and produces no pollution or noise. The low actuating voltage and quick bending responses of Ionic Conducting Polymer Film (ICPF) are considered very useful and attractive for constructing various types of actuators and sensors. In this paper, we will first study the characteristics of the ICPF actuator used in underwater microrobot to realize swimming and walking. Then, we propose a new prototype model of underwater swimming microrobot utilizing only one piece of ICPF as the servo actuator. Through theoretic analysis, the motion mechanism of the microrobot is illustrated. It can swim forward and vertically. The relationships between moving speed and signal voltage amplitude and signal frequency is obtained after experimental study. Lastly, we present a novel underwater crab-like walking microrobot named crabliker-1. It has eight legs, and each leg is made up of two pieces of ICPF. Three sample processes of the octopod gait are proposed with a new analyzing method. The experimental results indicate that the crab-like underwater microrobot can perform transverse and rotation movement when the legs of the crab collaborate.

Keywords: Underwater microrobot, Ionic Conducting Polymer Film (ICPF) actuator, motion mechanism, gait.

1 Introduction

Ion-based Ionic Conducting Polymer Films (ICPF), mostly belonging to the electro active polymers categories, have been investigated by researchers as possible materials for artificial muscles and MEMS actuators recently. The novel ICPF is becoming one of the most exciting ongoing research areas in Bio-MEMS, which paves the way to a great variety of biomimetic approaches for underwater microrobot design. The ICPF actuator consists of a perfluoro sulfonic acid membrane with chemically plated gold or platinum as electrodes on both sides. It bends by applying a low voltage between the electrodes. The actuator is soft and works in water and has a long life. It can respond quickly and bend silently. In particular, if the interstitial space of polyelectrolyte network is filled with liquid containing ions, then the electrophoresis migration of such ions inside the structure can also cause the macromolecular network to deform due to an imposed electric field^[1].

Actually the invention of underwater microrobot is expected to become increasingly popular in the applications of industrial, medical and military purposes. For example, maritime countries are gazing at underwater resource exploitation and water area domination. They pay attention to ocean environment research, ocean resource exploration, *etc.* Departments of both ocean exploitation and navy need underwater microrobot to carry out the work of underwater detection and exploration. Traditional underwater driving device adopts mode of screw propeller^[2] which has many defects, such as low efficiency of power, large size of structure and increase of more additional weight, high level of noise, low reliability and bad performance during start-up and acceleration. While the underwater microrobots including swimming microrobots and walking microrobots, which have been developed using biomimetic actuator, have many characteristics, such as maneuverability, efficiency, informatization, intellectualize and so on. For an industrial application, this kind of underwater microrobots can also be used in maintaining factory pipelines which are better than normal tools.

Theoretically, a microrobot using ICPF actuators has several advantages over other microrobots us-

Manuscript received July 10, 2006; revised August 29, 2006.

*Corresponding author. E-mail address:

yexiufen@hrbeu.edu.cn

ing SMA, GMA, PZT and other kinds of biomimetic actuator^[1,3~7]. One of them is the great possibility to work in a very small and dangerous space^[6,8,9]. Another is that the microrobot can be actuated with low power voltage. Moreover, it has many other advantages such as light weight, small structure, good input response, high security^[9,10], high efficiency of power transition^[10~12], little noise, fully energy utilization of surrounding medium, *etc.* Recently, many kinds of underwater microrobots have been developed for various purposes by using ICPF as the actuators^[1,13]. Biomimetic fish-like propulsion using double ICPF actuator as a propulsion tail fin for an underwater microrobot swimming structure in water or aqueous medium was developed^[14]. A type of micro biped robot with both walking and swimming motions has been researched^[15], which proved the swimming and floating possibility of the microrobot in water. A novel type of underwater microrobot utilizing just two segments of ICPF actuators shows that its crawling method has a good performance on rough surface^[16]. ICPF actuator is also used for biped walking underwater robot and multi-DOF manipulator^[17,18]. Inspired by walrus, a kind of walking microrobot using ICPF actuators has been designed and the speed of the microrobot has been measured with two methods^[19].

In this paper, we will firstly analyze the kinematics of ICPF actuator and then introduce a new kind of centimeter-sized underwater microrobot which can do forward, upward and downward movement freely like a shrimp by using only one piece of ICPF as the actuator. Lastly, we will introduce a crab-like walking underwater microrobot which has eight legs with altogether sixteen pieces of ICPF as the actuators. The experimental results indicate that the ICPF actuated microrobot can move as expected.

2 Kinematics analysis of ICPF actuator

As mentioned in the above section, ICPF would be useful as actuators to drive microrobot, one of our ongoing researches is to investigate the characteristics of ICPF actuator from the experiment.

2.1 Bending principle of ICPF actuator

The ICPF actuator is made of the film of perfluoro sulfonic acid polymer chemically plated on both of its sides with platinum (one side is 0.003 mm in thickness) as shown in Fig. 1. It is a kind of ion exchange film and can only work under water or in wet condition^[2,10]. Because the microcosmic structure of ICPF is ionization, in case it is affected by electric field, the ion included in the two sides of the polymer molecule chain will move to the cathode. At the same time, each ion could allure

some water molecules to move together to the cathode. Consequently, it causes the cathode of ICPF to expand and the anode to shrink so that the bend of ICPF is formed^[12,20]. The bending principle of ICPF is shown in Fig. 2. When adding an alternating voltage signal, the film would bend alternately. The bend displacement is decided by the voltage amplitude and frequency of the input signal. The other feature of the ICPF actuator is that when the frequency of the applied voltage signal is lower than 0.3 Hz, water around the ICPF surface is electrolyzed^[15]. It is possible for us to control the ICPF actuator by applying proper electrical voltage on the ICPF.

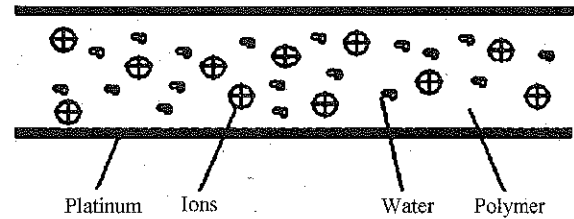


Fig. 1 Structure of ICPF actuator

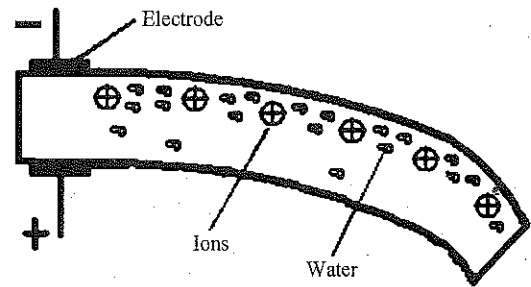


Fig. 2 Bending Principle of ICPF actuator

2.2 Analysis of the ICPF actuator

In order to study the kinematics characteristics of ICPF actuator, we set up experimental system as shown in Fig. 3. The size of the ICPF actuator is 15 mm in length, 5 mm in width and 0.15 g in weight. The input signal of the microrobot is produced by the computer and transformed to analog signal by D/A transformer (PIO-DA16). After that, the amplitude of the signal is magnified by going through the amplifier. A laser displacement sensor is used to measure the bending displacement d ^[21].

In the experiment, at first, we measure the bending displacement d of a piece of ICPF actuator by using the laser displacement sensor. Next, we will calculate the radius of curvature ρ of ICPF as shown in Fig. 4. One can compute ρ based on the displacement measurement d by using geometric theory:

$$[\rho - (d_0 - d)]^2 + h_0^2 = \rho^2 \quad (1)$$

$$\rho = \frac{\{(d - d_0)^2 + h_0^2\}}{2 \times (d_0 - d)} \quad (2)$$

where d_0 is the vertical distance from the laser sensor to the fixed end of ICPF and h_0 is the horizontal distance from the laser sensor to the fixed end of ICPF^[21]. L is the length of the ICPF actuator excluding the length of joints. From the above analysis, we know that the coordinates of the terminal point are influenced by the parameters ρ which can be calculated by (2).

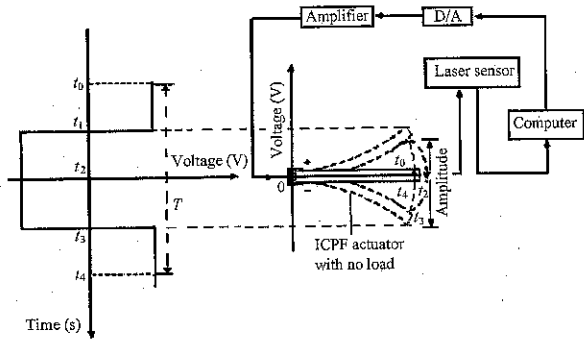


Fig. 3 Experimental system for displacement measurement of ICPF

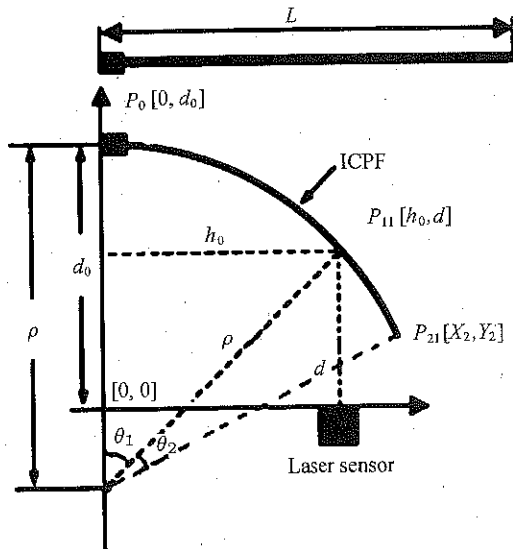


Fig. 4 Calculation of the radius of bending curvature ρ based on the parameter d when the ICPF is swinging down

The referenced frame is determined at the moment the ICPF actuator swings down, as shown in Fig. 4. In this figure, we define the point of P_{21} as the terminal of the ICPF actuator, and define the point of P_{11} as the point checked by the laser displacement sensor. Neglecting the influence of the joints, the analysis can precisely show the coordinates of P_{21} which is the terminal of the ICPF actuator. The coordinates of P_{21}

can be calculated as follows:

$$X_{21} = \rho \times \sin(\theta_1 + \theta_2) = \rho \times \sin\left(\frac{L}{\rho}\right) \quad (3)$$

$$Y_{21} = d_0 - \rho + \rho \times \cos\left(\frac{L}{\rho}\right) \quad (4)$$

As shown in Fig. 5, the referenced frame is determined at the moment the ICPF actuator swings up. We also define the point of P_{22} as the terminal of the ICPF actuator, and define the point of P_{12} as the point checked by the laser displacement sensor when the ICPF actuator is swinging up. Then, the coordinates of the point of P_{22} can be calculated as follows:

$$X_{22} = \rho \times \sin\left(\frac{L}{\rho}\right) \quad (5)$$

$$Y_{22} = \rho + d_0 - \rho \times \cos\left(\frac{L}{\rho}\right) \quad (6)$$

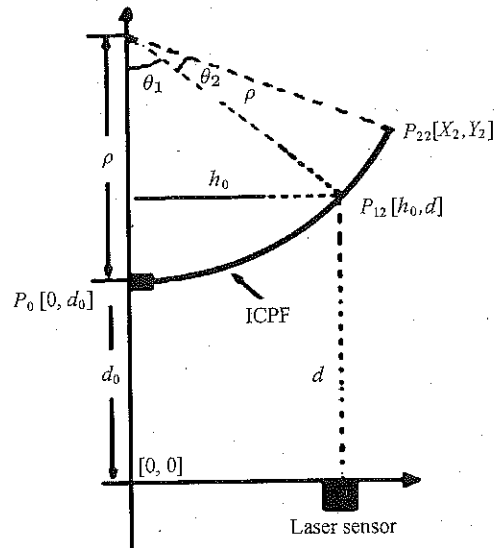


Fig. 5 Calculation of the radius of bending curvature ρ based on the parameter d when the ICPF is swinging up

The parameter ρ is related to the frequency and amplitude of the applied voltage at time t . As shown in Figs. 3~5, the parameter d is measured accurately by the laser displacement sensor. The diagram of minimum bending displacement d_{\min} under different voltages and frequencies is shown in Fig. 6, where d_{\min} is the distance between the point P_{11} and the X -axis when the ICPF swings down to the lower limit point and is measured by the laser displacement sensor. The diagram of maximum bending displacement d_{\max} under different voltages and frequencies is shown in Fig. 7, where d_{\max} is the distance between the point P_{12} and the X -axis when the ICPF swings up to the upper limit point and is measured by the laser displacement sensor.

The curve of bending displacement d vs. time under the control signal (5 V, 1 Hz) is shown in Fig. 8. According to the value of d , we can easily deduce ρ and calculate the coordinates of the terminal of the ICPF actuator P_2 by using (1)~(6).

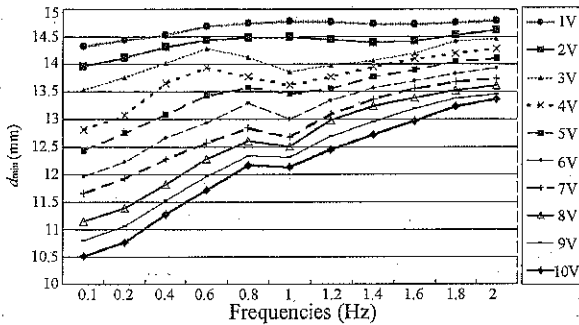


Fig. 6 Minimum bending displacement d_{min} of single ICPF under different voltages and frequencies

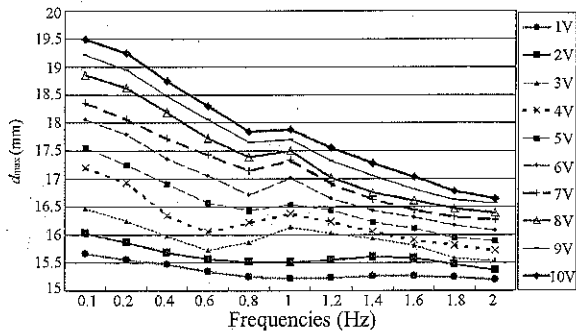


Fig. 7 Maximum bending displacement d_{max} of single ICPF under different voltages and frequencies

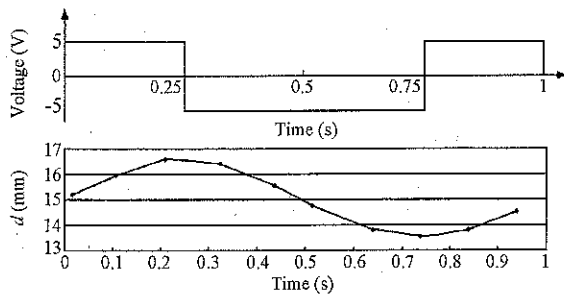


Fig. 8 Bending displacement d of single ICPF vs. time under different voltages and frequencies

The above analysis is just based on one piece of ICPF actuator. However, the kinematics mechanism analysis of a leg which is made up of double pieces of ICPF is also necessary. Now suppose that two pieces of ICPF with the same size are connected fixedly at a right angle. Fig. 9 shows four instances of the swing mechanism which are swung to different positions.

At the moment of case (2) in Fig. 10, we can deduce

the solution to the coordinates of point P_{32} from the following equations:

$$X_{32} = \rho_1 \times \sin\left(\frac{L}{\rho_1}\right) - \rho_2 \times \sqrt{2 - 2 \times \cos\left(\frac{L}{\rho_2}\right)} \times \cos\left(\frac{\pi}{2} - \frac{L}{\rho_1} + \frac{L}{2\rho_2}\right) \quad (7)$$

$$Y_{32} = d_0 - \rho_1 + \rho_1 \times \cos\left(\frac{L}{\rho_1}\right) - \rho_2 \times \sqrt{2 - 2 \times \cos\left(\frac{L}{\rho_2}\right)} \times \sin\left(\frac{\pi}{2} - \frac{L}{\rho_1} + \frac{L}{2\rho_2}\right) \quad (8)$$

where ρ_1 is the radius of curvature of the upper ICPF actuator, ρ_2 is the radius of curvature of the lower ICPF actuator. Actually, we neglect the influence of gravity of ICPF actuator which can have influence on the curvature of ICPF actuator and position of the terminal.

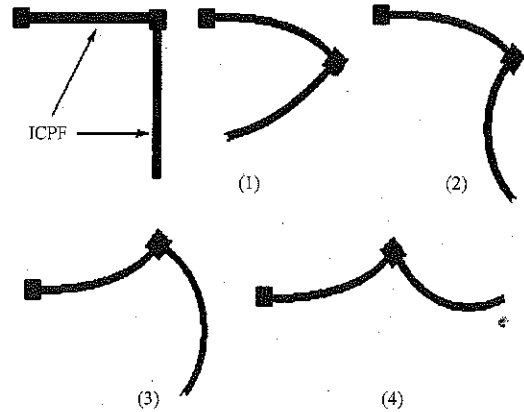


Fig. 9 Four instances of the swing mechanism

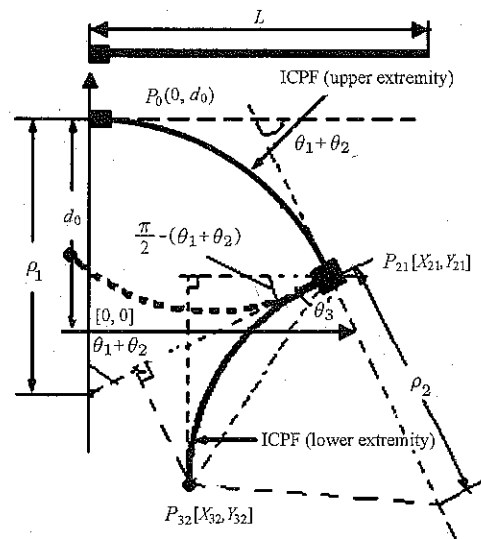


Fig. 10 Calculation on the coordinates of the P_{32} point at the moment of case (2)

3 Underwater swimming microrobot driven by single ICPF actuator

In this part, a kind of centimeter-sized underwater swimming microrobot is proposed, which uses only one piece of ICPF as the actuator. By input of proper control signals, it can do forward, upward and downward movement freely like a shrimp.

3.1 Structure of the swimming microrobot

As shown in Fig. 11, the microrobot comprises a main body, tail fin, flute, and ICPF actuator. The outside control signal is provided through the down-leads. The geometric structure of the microrobot is shown in Fig. 12. The wooden head of underwater microrobot with a streamline shape (Part A) is designed to reduce the resistance from water, just like a shrimp head. There are two electrodes embedded respectively in the shrimp body. The ICPF tail fin is fixed into the shrimp body and is taken as the driving device just like the tail of shrimp. The rearward of the microrobot is made of plastic and is shaped in flute (Part C) and the bottom part is ICPF actuator (Part E) with a rearward tail fin (Part B) to make the impetus more effectively. The flute is not only used to extrude water by cooperating with the tail fin, but also used to keep the balance of the microrobot in the water. The specifications of the microrobot are shown in Table 1.

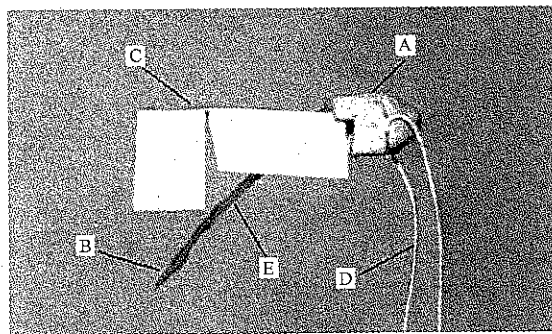


Fig. 11 Basic structure of the underwater microrobot
A: Main body, B: Tail fin, C: Flute, D: Down-lead,
E: ICPF

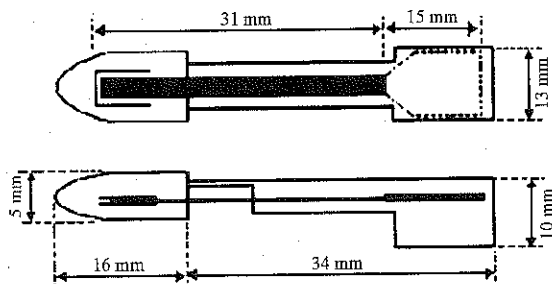


Fig. 12 Geometric structure of the microrobot

Table 1. Specifications of the prototype microrobot

Size	50 mm×13 mm×10 mm
Weight	1.9 g
Material of body	Wood
Material of flute	Plastic
Actuator	31 mm×5 mm×0.3 mm ICPF bar
Power supply range	2 V~10 V AC (frequency from 0.2 Hz to 2 Hz)

3.2 Principle of swimming and control signal

The above proposed microrobot can accomplish the movement of swimming forward, sinking down and floating upward. The mechanism of motion in water is introduced as follows:

1) Motion of moving forward:

When applying periodic alternating voltage signal on the ICPF, it will swing periodically. The fin can extrude water by cooperating with the plastic flute and produce driving force on the microrobot. However, when the tail fin bends downwards, there will be a backward resistance to counteract the forward motion of the microrobot. In order to reduce the resistance brought by the tail fin when swinging downwards and to obtain a better swimming speed, we must control the waveform of the input control signal according to biomimetic rule, so that the trapezium shaped voltage waveform is used as the input signal, as shown in Fig. 13.

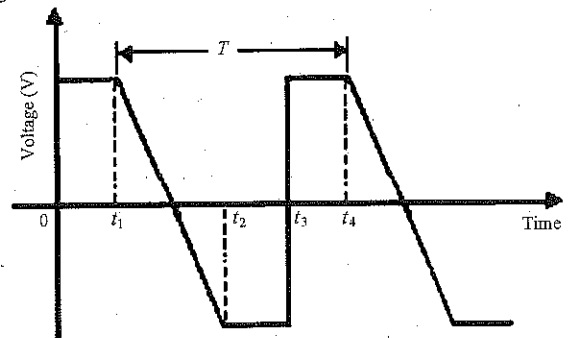


Fig. 13 Waveform of input voltage to drive forward

When applying voltage signal range from 2 V to 10 V on the ICPF actuator as shown in Fig. 13, the tail fin of the microrobot will swing and drive the microrobot to move. When the tail fin swings up, it clamps the flute, thus backward cascade is produced and the consequent retroaction force pushes the microrobot forward. The dynamical mechanism of pushing forward can be expressed as^[10]

$$F_d = -\frac{1}{2}C_d\rho AV_h|V_h| \quad (9)$$

where C_d is the drag coefficient based on wet surface

area A , ρ is the density of water, V_h is the relative speed between the surface of the microrobot and the water.

There are three procedures in a motion period T of the ICPF shown in Fig. 13: From t_1 to t_2 , the tail fin swings downwards. The changing process of voltage from positive to negative is slow, so that when the tail fin swings downwards, the counterforce by water to the tail fin can be greatly reduced. From t_2 to t_3 , the tail fin keeps swinging downwards, this movement makes a proper displacement between the tail fin and the flute. The displacement is large enough for ICPF actuator to scrape up energy for swinging upwards. At this stage, the ICPF actuator is actually pushing water to make the microrobot move back, and at the same time engendering a counterforce of buoyancy. From t_3 to t_4 , the value of voltage changes from negative to positive swiftly, consequently the tail fin swings upwards rapidly and makes a water extrusion movement with the flute and engenders backward cascade. This pushes the robot to swim forward in a faster speed. The advantage of this kind of trapezoid shape voltage waveform is that the ICPF swings downwards slowly and swings upwards swiftly, therefore the impetus can more efficiently push the microrobot to move forward with little fore-and-aft dither. Moreover, we can change the speed of microrobot by changing the slope and amplitude of the trapezoid shape waveform.

Fig. 14 shows the underwater swimming microrobot moving forward on the surface of water. Fig. 15 shows the diagram of moving speed under different voltages and frequencies (the voltage is ranged from 5 V to 9 V and the frequency range is from 0.5 Hz to 2.0 Hz). The curve in Fig. 15 shows that the speed of microrobot swimming on the surface of water increases along with the voltage of input signal, and gets a max speed when the frequency of input signal is 1 Hz.

2) Motion of floating upward:

Fig. 16 shows the signal for the microrobot to move upwards, which is different from the signal for driving forwards. The tail fin swings upward during the time from t_1 to t_2 . Then the tail fin swings downwards rapidly during the time from t_2 to t_3 with the swift change of voltage from positive to negative. Consequently the water will produce a force F on the tail fin, as shown in Fig. 17. In fact, the transverse component of F (force F_x) is a force that can prevent the microrobot from moving forward. However, in the process of the tail fin moving downward, the microrobot can still move forward by inertia force. The longitudinal component force F_y is a kind of Buoyancy Force. Fig. 18 shows a picture of the microrobot floating upward. The background is a frame of reference which is separated into 1 cm width and 1 cm height squares. When we

remove the signal applied on the ICPF actuator, the robot can sink down only by its weight.

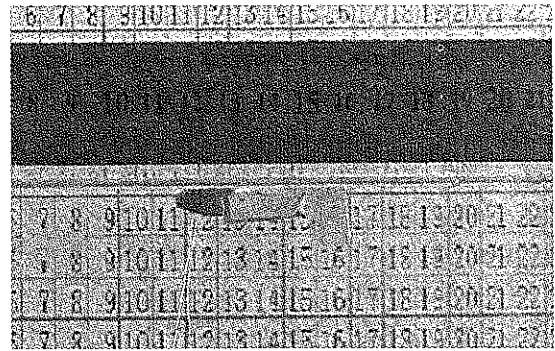


Fig. 14 Moving forward of the microrobot on the surface of water

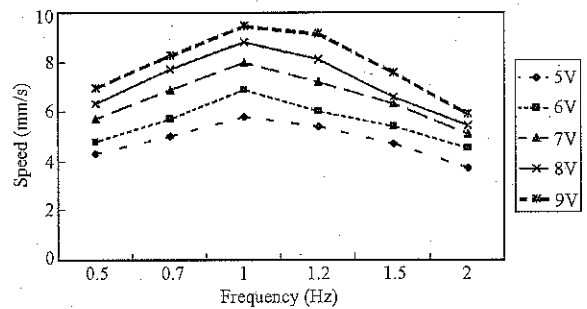


Fig. 15 Moving speed under different voltages and frequencies

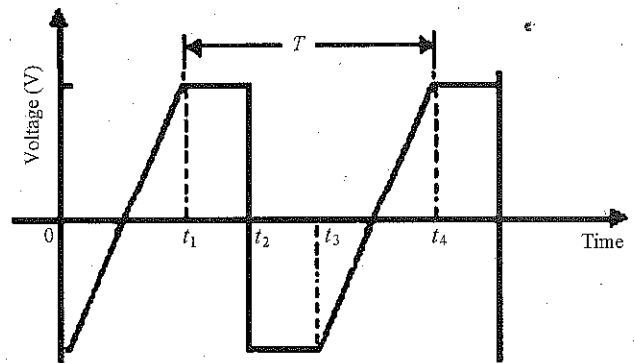


Fig. 16 Waveform of input voltage

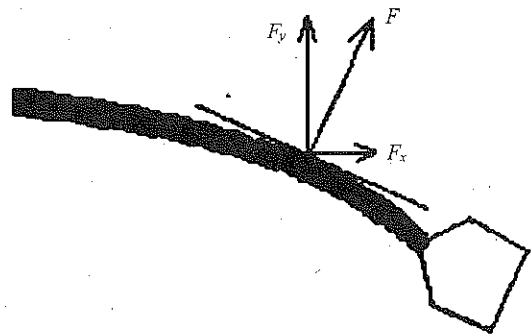
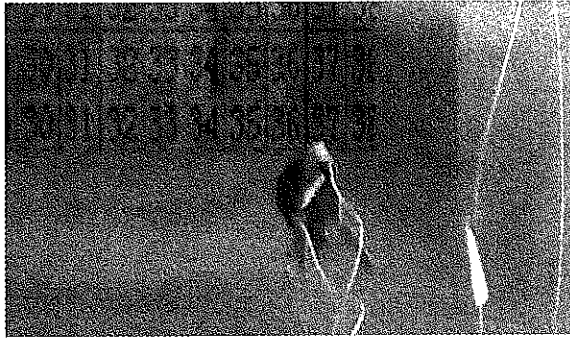
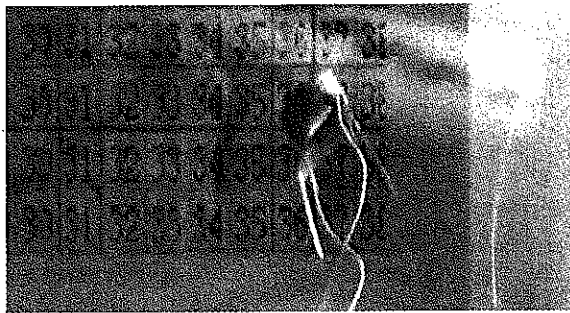


Fig. 17 Forces on tail fin when moving downwards



(a) Initial position of the floating motion



(b) One picture of the micro-robot at the moment of floating upward

Fig. 18 A picture of the micro-robot floating upward

4 Underwater crab-like walking micro-robot

Another underwater walking micro-robot named crabliker-1 is also proposed, which has eight legs, and each leg is made up of two pieces of ICPF.

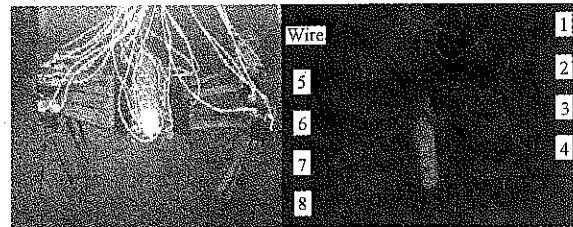
4.1 Structure of the crab-like micro-robot

Walking robots provide flexible adaptive mobility in unstructured environment or in unpredictable dynamic surrounding with the help of servo controlled legs^[22]. Crab has five pairs of thoracic feet as shown in Fig. 19(a). The terminal of the first pair look like tongs, which is named as griddle feet, mostly designed to defend and attack, the last four pairs have the general name of walking legs. Walking legs droop and are arranged compactly. Their distribution extend to both sides of the crab. Thus, the crab could do lateral movement with low cg and good stability. Every segment plays different role in crab's moving action. Inspired by crab, a micro-robot, named Crabliker-1, is designed and realized. The basic structure of the underwater walking micro-robot using ICPF actuator is shown in Fig. 19(b). Crabliker-1 is 35 mm in length, 40 mm in width, 22 mm in height and 4.5 g (dried) in weight. It has eight legs and each one has two segments of ICPF

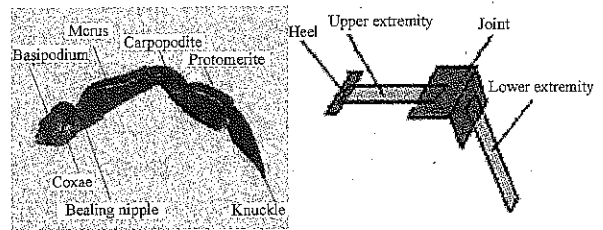
actuators jointing at a right angle nearly. Fig. 19(c) shows the structure of a single leg compared with the walking leg of the crab. The crawling leg of the crab comprises basipodium, coxae, seating nipple, merus, carpopodite, protomerite and knuckle. The single leg we designed comprises heel, upper extremity, joint and lower extremity. The heel plays the role of permanent connection on the main body of micro-robot, just like the segment of basipodium. The upper extremity is a piece of ICPF actuator, which realizes the phase of swing that pushes the main body up when swinging down and raises the leg up when swinging up. The part of joint is used to join the lower extremity to upper extremity and forms a right angle between them. The lower extremity is also made by ICPF actuator and realizes the phase of support of the micro-robot and swing to perform transverse and rotation movement.



(a)



(b)



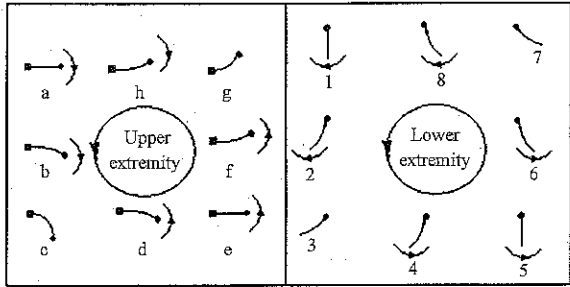
(c)

Fig. 19 Structure of crab compared with the micro-robot

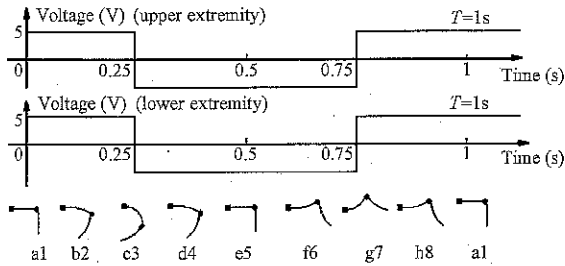
4.2 Analysis of gait of the crab-like micro-robot

Through analysis of the ICPF actuator in the above section, we define the eight states of the upper extrem-

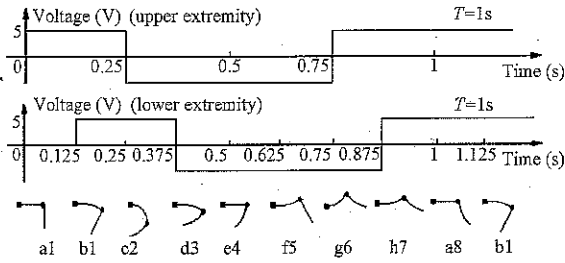
ity from 'a' to 'h' and define the eight states of the lower extremity from '1' to '8', as shown in Fig. 20(a). There are 64 states which the single leg can have in this paper. They are named separately from 'a1' to 'h8'. In order to analyze the gait of the microrobot exactly, we give serial number to each single leg in Fig. 19(b). Then we use different type of lines to express the different phases of the single leg's movement in octopod gait analyzing.



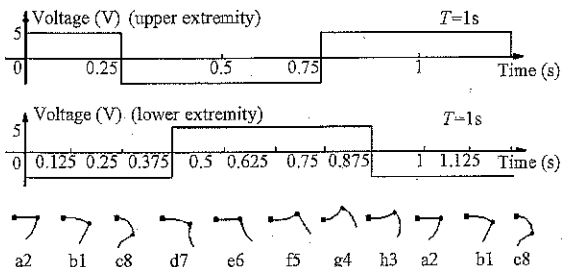
(a)



(b)



(c)



(d)

Fig. 20 Process of the single leg's movement

In the experiment, we have tried different ways to

control the gait of the microrobot based on the observation of crab's gait, and at last we find the way for the microrobot to carry out the lateral movement and plane turn movement successfully. Fig. 20 gives three different control signal waveforms (5 V, 1 Hz) applying to the different legs of the microrobot, which plays different roles on the main body of the microrobot. Three different phases can be explained as follows:

1) Phase A: In this phase, the single leg has a strong propulsive force on the ground which pushes the microrobot rightward, such as, the states of 'a1' to 'c3' in Fig. 20(b) and the states of 'a8' to 'c2' in Fig. 20(c). They both play the same role of pushing the microrobot rightward. It takes one quarter of a cycle totally for this phase and can be expressed by the black thick line in Figs. 21 and 22.

2) Phase B: As shown in Fig. 20(b), the states from the states of 'c3' to 'e5' play the role of sustaining the microrobot stably. It takes one quarter of a cycle totally for this phase and can be expressed by the black thin line in Figs. 21 and 22.

3) Phase C: In this phase, the single leg swings up and has no contact with the ground and swings the whole leg up. We also define it the phase of adjustment. Such as, the states from the states of 'e5' to 'h8' in Fig. 20(b), the states of 'd3' to 'h7' in Fig. 20(c) and the states of 'e6' to 'a2' in Fig. 20(d). It takes half of a cycle totally for the adjustment phase and can be expressed by the gray thick line in Figs. 21 and 22.

4) Phase D: In this phase, the single leg has a strong force on the ground, but the force is different from the one in Phase A in that the direction of the force is opposite to the force in phase A, so the single leg has reverse effect on the body of the microrobot. Such as, the states from the states of 'a8' to 'c2' in Fig. 20(c), it takes one quarter of a cycle totally for this phase and can be expressed by the black broken line in Figs. 21 and 22.

Fig. 21 shows the gait of the microrobot when moving rightwards and Fig. 22 shows the gait of the microrobot when moving circumvolve anticlockwise. Both of the above motion modes of the gait are carried out under the control signal (5 V, 1 Hz). Fig. 23(a) shows that the microrobot is located in the initial point, and Fig. 23(b) presents that the microrobot is moving rightward when the control instruction to move rightward is applied, and the Fig. 23(c) shows the state of the circumvolve anticlockwise of microrobot when the control instruction to turn the microrobot to the left is applied. The results prove the gaits proposed are feasible.

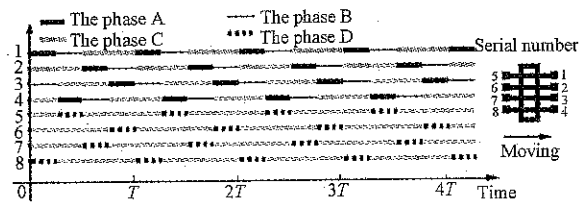


Fig. 21 Gait of the microrobot when moving rightwards

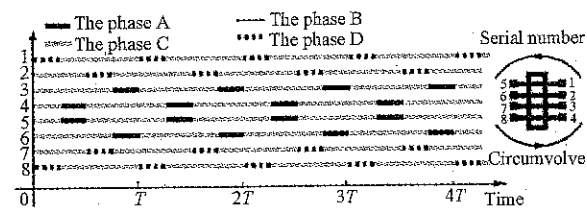


Fig. 22 Gait of the microrobot when moving circumsolve anticlockwise

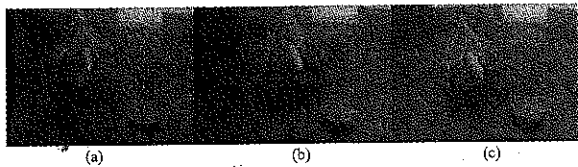


Fig. 23 Process of the microrobot's movement

5 Conclusions

In this paper, a new type of swimming underwater microrobot using single piece of ICPF as the actuator and a novel crablike underwater walking microrobot named crabliker-1 are proposed. And we have discussed the characteristics of ICPF actuator by setting up the experimental platform. Based on this analysis, we apply a trapezia shape voltage control signal on the swimming microrobot. We also propose three processes of the single leg's movement under different control signals applied on the crab-like underwater microrobot. At last, we introduce the microrobot's gait of carrying out the rightwards movement and gait of carrying out circumsolve anticlockwise. The experimental results indicate that the amplitude of swing and angular velocity as well as proper underwater microrobot movement can be controlled by changing the frequency and the amplitude of input voltage.

More improvements and more progresses are expected in the related fields of centimeter-sized underwater swimming and walking microrobot in the future. In our future work, we will study the coordinate control algorithm among legs and the swimming mechanism of the crabliker-1 microrobot. We will also continue the work in developing new usages of ICPF actuator in medical field and in medical and industrial appli-

cations and continue the work in further studying the kinematics and dynamics characteristics of the ICPF actuator.

References

- [1] M. Mojarrad, M. Shahinpoor. Biomimetic Robotic Propulsion Using Polymeric Artificial Muscles. In *Proceedings of the 1997 IEEE International Conference on Robotics and Automation*, Albuquerque, New Mexico, pp. 2152–2157, April 1997.
- [2] S. Guo, T. Fukuda, K. Oguro. Development of an Artificial Fish Microrobot. In *Proceedings of the International Symposium on Micromechatronics Human Science Nagoya Congress Center*, Nagoya Municipal Industrial Research Institute, Japan, pp. 135–140, November 23–26, 1999.
- [3] T. Fukuda, K. Hosokai, F. Arai. Giant Magnetostrictive Alloy (GMA) Applications to Micro Mobile Robot as a Micro Actuator without Power Supply Cables. In *Proceedings of IEEE Conference on Micro Electro Mechanical Systems*, Interlaken, Switzerland, pp. 210–215, 1990.
- [4] T. Fukuda, H. Hosokai, I. Kikuchi. Distributed Type of Actuator by Shape Memory Alloy and Its Application to Underwater Mobile Robotic Mechanism. In *Proceedings of IEEE International Conference on Robotics and Automation*, Nara, Japan, vol. 2, pp. 1316–1332, 1991.
- [5] L. Fearing. Micro Structures and Micro Actuators for Implementing Sub-millimeter Robots. *Precision Sensors, Actuators and Systems*, Kluwer Academic Publishers, Boston, MA, pp. 39–72, 1992.
- [6] T. Fukuda, A. Kawamoto, F. Arai. Steering Mechanism of Underwater Micro Mobile Robot. In *Proceedings of IEEE International Conference on Robotics and Automation*, Nagoya, Japan, vol. 1, pp. 363–368, May 1995.
- [7] T. Fukuda, A. Kawamoto, F. Arai, H. Matsuura. Mechanism and Swimming Experiment of Micro Mobile Robot in Water. In *Proceedings of IEEE International Conference on Robotics and Automation*, New Orleans, LA, USA, vol. 1, pp. 814–819, 1994.
- [8] Y. Hirose, T. Shiga, A. Okada, T. Kurauchi. Gel Actuators Driven by an Electric Field. In *Proceedings of 3rd International Symposium on Micro Machine and Human Science*, Nagoya, Japan, pp. 21–26, 1992.
- [9] S. Guo, T. Fukuda, N. Kato, K. Oguro. Development of Underwater Microrobot Using ICPF Actuator. In *Proceedings of the 1998 IEEE International Conference on Robotics and Automation*, Leuven, Belgium, pp. 1829–1834, May 1998.
- [10] S. Guo, T. Fukuda, K. Asaka. Fish-like Underwater Microrobot with 3 DOF. In *Proceedings of IEEE International Conference on Robotics and Automation*, Washington, USA, pp. 738–743, May 2002.
- [11] S. Guo, Y. Okuda, K. Asaka. Characteristic Evaluation of an Underwater Micro Biped Robot with Multi DOF. In *Proceedings of the 2004 International Conference on Intelligent Mechatronics and Automation*, Chengdu, China, pp. 95–100, August 2004.
- [12] H. Okuzaki, Y. Osada. Effects of Hydrophobic Interaction on the Cooperative Binding of Surfactant to a Polymer Network. *Macromolecules*, vol. 27, no. 2, pp. 502–506, 1994.
- [13] M. Shahinpoor, Y. Bar-Cohen, J. O. Simpson, J. Smith. Ionic Polymer-Metal Composites (IPMC) as Biomimetic Sensors, Actuators and Artificial Muscles—A Review. *International Journal of Smart Materials and Structures*, vol. 7, no. 6, pp. R15–R30, 1998.
- [14] S. Guo, T. Fukuda, K. Asaka. A New Type of Fish-like Underwater Microrobot. *IEEE/ASME Transactions on Mechatronics*, vol. 8, no. 1, pp. 738–743, March 2003.

- [15] S. Guo, Y. Okuda, K. Asaka. Hybrid Type of Underwater Micro Biped Robot with Walking and Swimming Motions. In *Proceedings of IEEE International Conference on Mechatronics and Automation*, Niagara Falls, Canada, vol. 3, pp. 1604–1609, July 2005.
- [16] W. Zhang, S. Guo, K. Asaka. Developments of Two Novel Types of Underwater Crawling Microrobots. In *Proceedings of The IEEE International Conference on Mechatronics and Automation*, Niagara Falls, Canada, vol. 4, pp. 1884–1889, July 2005.
- [17] N. Kamamichi, Y. Kaneda, M. Yamakita, K. Asaka, Z. W. Luo. Biped Walking of Passive Dynamic Walker with IPMC Linear Actuator. In *Proceedings of SICE Annual Conference 2003*, Fukui, Japan, pp. 212–217, August 2003.
- [18] Y. Nakabo, T. Mukai, K. Asaka. A Multi-DOF Robot Manipulator with a Patterned Artificial Muscle. In *Proceedings of the Second Conference on Artificial Muscles*, Osaka, Japan, 2004.
- [19] W. Zhang, S. Guo. The Development of a New Kind of Underwater Walking Robot. In *Proceedings of International Conference on Complex Medical Engineering*, Takamatsu, Japan, pp. 199–204, 2005.
- [20] M. Otake, Y. Kagami, Y. Kuniyoshi, M. Inaba, H. Inoue. Inverse Dynamics of Gel Robots made of Electro-active Polymer Gel. In *Proceedings of the 2003 IEEE International Conference on Robotics and Automation*, Taipei, vol. 2, pp. 2299–2304, September 14–19, 2003.
- [21] Z. Chen, X. Tan, M. Shahinpoor. Quasi-static Positioning of Ionic Polymer-Metal Composite (IPMC) Actuators. In *Proceedings of the 2005 IEEE/ASME International Conference on Advanced Intelligent Mechatronics Monterey*, California, USA, pp. 60–65, July 24–28, 2005.
- [22] O. C. How, S. H. M. Amin. Biologically Inspired Hybrid Three Legged Mobile Robot. In *Proceedings of The Student Conference on Research and Development*, Shah Alam, Malaysia, pp. 181–183, July 16–17, 2002.



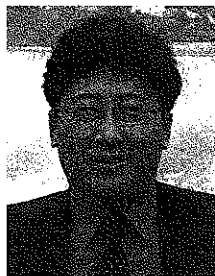
Xiu-Fen Ye received her B.S. degree in automation and the M.Sc degree in control theory and application from Harbin Shipbuilding Engineering Institute, Harbin, China in 1987 and 1990, respectively and the Ph.D. degree in control theory and control engineering from Harbin Engineering University, Harbin, China in 2003. She is currently a professor in the Lab of Biomimetic Micro Robot and System, Harbin Engineering University, China.

She has published over 40 journal and conference papers. Her current research interests include biomimetic microrobot system, network computing, image processing and pattern recognition.



Harbin, China.

His research interests include micro robotics and automation, especially the control of micro robotics such as gait control of underwater microrobot.



Japan. Currently, he is a professor in the Department of Intelligent Mechanical System Engineering at Kagawa University.

He has published about 140 refereed journal and conference papers. His current research interests include micro robotics and mechatronics, micro robotics system for minimal invasive surgery, micro catheter system, micro pump, and smart material (SMA, ICPF) based on actuators.

Prof. Guo received research awards from the Tokai Section of the Japan Society of Mechanical Engineers (JSME), the Tokai Science and Technology Foundation, and the Best Paper Award of the IS International Conference, Best Paper Award of the 2003 International Conference on Control Science and Technology and Best Conference Paper Award of IEEE ROBIO2004, in 1997, 1998, 2000, 2003 and 2004, respectively.

Bao-Feng Gao was born in Liaoning, China in 1981. He received his B.Sc. degree in forest engineering (international engineering project management) from the Northeast Forest University, Harbin, China in 2003. He is currently pursuing his M.Sc degree in control theory and control engineering from the Lab of Biomimetic Micro Robot and System, College of Automation, Harbin Engineering University,

Shu-Xiang Guo received his B.S. and the M.S. degrees in mechanical engineering from the Changchun Institute of Optics and Fine Mechanics, Changchun, China in 1983 and 1986, respectively, and the Ph.D. degree in mechano-informatics and systems from Nagoya University, Nagoya, Japan in 1995. In 1995, he was a faculty member at Mie University, Mie, Japan and in 1998 at Kagawa University, Kagawa,

International Journal of Automation and Computing

International Journal of Automation and Computing (ISSN 1476-8186) is a joint publication of Institute of Automation, Chinese Academy of Sciences and Chinese Automation and Computing Society in the United Kingdom.

Prof. T N Tan
Institute of Automation
Chinese Academy of Sciences
Beijing 100080
People's Republic of China
Email: tnt@nlpr.ia.ac.cn

Editors-in-Chief
Prof. G P Liu
School of Electronics
University of Glamorgan
Pontypridd CF37 1DL
United Kingdom
Email: gpliu@glam.ac.uk

Prof. H Hu
Department of Computer Science
University of Essex
Colchester CO4 3SQ
United Kingdom
Email: hhu@essex.ac.uk

Editorial Advisory Board

Prof. D E Brown, Virginia University, USA
Prof. H F Chen, Chinese Academy of Sciences, PRC
Prof. R W Dai, Chinese Academy of Sciences, PRC
Prof. S Daley, University of Sheffield, UK

Prof. G W Irwin, Queen's Univ. of Belfast, UK
Prof. S D Ma, Chinese Academy of Sciences, PRC
Prof. D T Pham, University of Wales, UK
Prof. T J Tam, Washington Univ. in St. Louis, USA

Editorial Board

Prof. P Blazevic, Universite de Versailles, France
Dr. J Bullinaria, University of Birmingham, UK
Prof. B Chen, University of Warwick, UK
Prof. K Cheng, Leeds Metropolitan University, UK
Dr. F Dewhurst, University of Manchester, UK
Prof. G R Duan, Harbin Institute of Technology, PRC
Prof. L Guo, Chinese Academy of Sciences, PRC
Prof. J M Jiang, University of Bradford, UK
Prof. H K Kolowrocki, Maritime University, Poland
Dr. C Kambhampati, University of Hull, UK
Prof. R G Roberts, Florida State University, USA
Dr. P P Smith, University of Oxford, UK

Prof. M Tan, Chinese Academy of Sciences, PRC
Prof. J Wang, Liverpool John Moores University, UK
Prof. H Wang, University of Manchester, UK
Dr. J F Whidborne, King's College London, UK
Prof. Q H Wu, Liverpool University, UK
Prof. A K Verma, Indian Institute of Tech., Bombay, India
Prof. H J Yang, De Montfort University, UK
Prof. J B Yang, University of Manchester, UK
Prof. X Yao, University of Birmingham, UK
Prof. Z X Zhao, University of Derby, UK
Prof. Y Yagi, University of Osaka, Japan

Guidelines for Authors

The International Journal of Automation and Computing (IJAC) publishes papers on original theoretical and experimental research and development in automation and computing. The scope of the journal is extensive. Topic includes but is not limited to: Artificial intelligence, Automatic control, Bio-informatics, Computer science, Information technology, Modelling and simulation, Networks and communications, Optimisation and decision, Pattern recognition, Robotics, Signal processing, Systems engineering.

Submission of papers

Please log on IJAC website: <http://www.ijac.net> to submit your papers. Papers must be in English. All submissions are acknowledged. DOC, PDF or PS files that are ready to be printed can be accepted.

Conditions of publication: It is a condition of publication that manuscripts submitted to *IJAC* have not been published and will not be submitted or published elsewhere in English or any other language, without the written consent of the publisher. Responsibility for the contents of the paper rests upon the authors and not upon *IJAC*, the Editors, or the Publisher.

Types of contribution

Submitted articles may be of three basic types:

Regular papers: Detailed discussion involving new research, applications or developments;

Brief papers: Brief presentations of new technical concepts and developments;

Correspondence: Letters to the Editor about the journal or to authors commenting on previously published papers. In the latter case, the Editor will give the authors an opportunity to respond.

Manuscript preparation

General: Manuscripts must be printed in double-column single-spaced format with wide margins on one side of A4 white paper. High quality printouts with a font size of 12pt or 10pt are required. The fax number, e-mail address, and postal address of the corresponding author, who should easily be identified with an asterisk and footnote, should be given. Full postal addresses of all co-authors must be included.

Text: Manuscripts should include the following parts (in order): Title, Authors, Affiliations, Abstract, Keywords, Main text, Fund and its number that support the paper if available, Appendices, References and Biographies.

References: All publications cited in the text should be presented in the reference list at the end of the manuscript. References must be listed in the order they were cited (numerical order). It is not necessary to mention the author(s) of the reference unless it is relevant to your text. The names of all authors should be given in the references unless the number of authors is greater than six. If there are more than six authors, you may use et al. after the name of the first author. An example of references is given below:

[1] D. Xu, M. Tan, X. G. Zhao, Z. G. Tu. Seam Tracking and Visual Control for Robotic Rrc Welding Based on Structured Light Stereovision. *International Journal of Automation and Computing*, vol.1, no.1, pp. 63-75, 2004

Illustrations: All illustrations must be provided in a camera-ready form, which are suitable for reproduction. Photographs, charts and diagrams are all to be referred to as "Figure(s)" and should be numbered consecutively in the order to which they are referred. They should be included within the text. Every figure must have a caption.

Tables: Tables should be numbered consecutively with suitable captions.

Biographies: A short biography and the photograph of every author should be provided for regular papers and brief papers.

Copyright

All authors must sign the Transfer of Copyright Agreement before the paper can be published. This agreement enables the Publisher to protect the copyrighted material for the authors without affecting the authors' proprietary rights. Authors are responsible for obtaining permission from the copyright holder to reproduce any figures or other material included in the paper for which copyright already exists.

Author Enquiries

For enquiries relating to the submission of papers, the status of accepted papers, author frequently asked questions, please consult Editorial Office. Contact details for questions arising after acceptance of an article, especially those relating to proofs, are provided when an article is accepted for publication.

Statement

The prerequisite of publication is that manuscripts submitted to IJAC have not been published and will not be submitted or published elsewhere in English or any other language, without the written consent of the Editorial Office of International Journal of Automation and Computing. Responsibility for the contents of the paper rests upon the authors and not upon IJAC, the Editors, or the Publisher.

International Journal of Automation and Computing

Vol.3 No.4 October 2006 (Quarterly, Started in 2004)

Edited by: Editorial Board of International Journal of Automation and Computing

Editors-in-Chief: T N Tan, G P Liu, H Hu

Managed by: Chinese Academy of Sciences

Sponsored by: Institute of Automation, Chinese Academy of Sciences

Published by: Science Press, Beijing, PRC

Printed by: Beijing Kexin Printing House

Distributed by: Science Press, Beijing, PRC

Managing Editor: F Fu

Editorial Office:

Institute of Automation, Chinese Academy of Sciences, P.O.Box 2728, Beijing 100080, PRC

Telephone: +86 10 62655893 Fax: +86 10 82614571 E-mail: ijac@ia.ac.cn <http://www.ijac.net>

All rights reserved. No part of this publication may be reproduced, stored in a retrieval system, or transmitted in any form or by any means, electronic, mechanical, photocopying, recording or otherwise, without the written consent of the copyright owner.

Copyright © 2006 by Editorial Office of International Journal of Automation and Computing

CN11-5350/TP

Domesite distribution postcode: 80-479

RMB¥ 50.00

ISSN 1476-8186

